Reaction and surface characterization studies of Ru/Al_2O_3 catalysts for CO preferential oxidation in reformed gas

Mitsuaki Echigo* and Takeshi Tabata

Residential Cogeneration Development Department, Osaka Gas Co., Ltd., 3–4, Hokko Shiratsu 1-chome, Konohana-ku, Osaka 554-0041, Japan

Received 23 April 2004; accepted 6 August 2004

In order to investigate the reasons the activation of a Ru/Al_2O_3 catalyst by heating in a H_2/N_2 mixed gas improves the CO preferential oxidation (PROX) activity, the oxidation state of the Ru on the catalyst surface was studied by using ESCA. As the ratio of Ru(0) to total Ru on the surface was increased, the temperature window of the Ru catalyst, where CO was reduced to below 10 ppm, was expanded to the lower temperature side. The activity of CO oxidation by O_2 of the Ru catalyst at lower temperatures was improved by increasing the ratio of Ru(0). However, the selectivity for CO oxidation hardly varied with the change in the surface Ru(0) ratio at these low temperatures. It is considered that O_2 activation on Ru(0) plays an essential role in CO PROX activity on the Ru catalyst at low temperatures.

KEY WORDS: CO preferential oxidation, ESCA, polymer electrolyte fuel cell, PROX, reformed gas, Ru catalyst.

1. Introduction

The hydrogen-rich reformed gas from hydrocarbons like natural gas is a convenient fuel for stationary PEFC systems, such as in residential use. The natural gas reforming process, comprising a desulfurizer, a steam reformer and a CO shift converter, has already been established for the Phosphoric Acid Fuel Cell (PAFC) system [1–3]. The reformed gas after the CO shift converter contains about 0.5 vol.% CO. This CO concentration is acceptable for the anode catalyst of the PAFC operated at ca. 473 K. On the other hand, the anode catalyst of the PEFC is poisoned by only 10 ppm CO, because the operation temperature of the PEFC is ca. 353 K [4–6]. Although CO-tolerant anode catalysts containing Ru in addition to Pt have been developed for the PEFC [7–9], the acceptable CO concentration of the anode catalyst appears to be ca. 10 ppm considering long-term durability. Therefore, for a PEFC system using natural gas, a CO removal process is required in addition to the reforming process established for the PAFC.

Generally, a CO preferential oxidation (PROX) using Pt-based catalysts has been used for the CO removal process. It was reported that CO was reduced to ca. 100 ppm on a Pt/Al_2O_3 catalyst with the addition of excess air corresponding to $[O_2]/[CO] = 2$ [4]. It has also been reported that the additive air corresponding to $[O_2]/[CO] > 3$ was needed to remove CO completely on a conventional Pt/Al_2O_3 catalyst [10]. The excess O_2 consumes H_2 in the reformed gas by combustion, which causes a decrease in the power generation efficiency of the PEFC system. Therefore, a multi-stage CO PROX has been mainly adopted in actual reactors [11–16] because the total amount of additive air can be reduced by optimizing the additive air at each stage. It has been reported that CO was reduced to less than 10 ppm by a two-stage reactor at a total additive air corresponding to $[O_2]/[CO] = 1.5$ [16]. However, complex hardware is required to control the temperatures and oxidant injections along the multi-stage catalytic layer. Meanwhile, several kinds of the Pt-based catalysts have been studied to improve the selectivity and activity for CO oxidation [10–24]. However, their performance in an actual reactor and the long-term durability have not been demonstrated.

On the other hand, some reports show that Ru catalysts have a wider temperature window for CO PROX than Pt catalysts [7–27]. It has been reported that CO was reduced to below 100 ppm at ca. 468–503 K on a Ru catalyst, while at ca. 463–473 K on a Pt catalyst under the experimental conditions of $H_2/CO/CO_2/O_2 = 75/1/25/1.5$ and SV = 6,500 h^{-1}. The minimum outlet CO concentrations of the Ru catalyst appeared to be ca. 50 ppm at ca. 483 K [26]. It has also been reported that CO was reduced to below 100 ppm at the reactor temperature of ca. 412–418 K and the minimum outlet CO concentration appeared to be ca. 80 ppm at ca. 415 K, when the CO preferential oxidation was carried out on a Ru catalyst at $[O_2]/[CO] = 1.25$ and GHSV = 4,800 h^{-1} [27]. On the other hand, Ru catalyst also possesses considerable methanation activity [28]. Because temperature control is quite difficult in actual reformate due to self-catalytic endothermic CO_2 methanation, a Ru catalyst is seldom used solely except for use in the second stage of the two-stage CO PROX.

* To whom correspondence should be addressed.

1011-372X/04/1000–0037/0

In a previous work, we reported that the novel Ru catalyst, which was obtained by activating a Ru/Al_2O_3 in an H_2/N_2 mixed gas after aqueous reduction, had extremely high practical CO PROX performance even at a single-stage reactor for residential PEFC applications. On the catalyst, CO was reduced from 0.5 vol.% to below 10 ppm between 363 K and 413 K at $[O_2]/[CO] = 1.0$ and between 358 K and 443 K at $[O_2]/[CO] = 1.5$ in a simulated reformed gas [29]. The novel Ru catalyst has already been used practically, and its durability has been demonstrated over 10,000 h in an actual 1 kW-class natural gas fuel processor adopting a single-stage CO PROX reactor [30]. In this paper, in order to investigate the reason the activation improved the CO PROX activity, the oxidation state of the Ru was studied by using ESCA.

2. Experimental

Ru/Al_2O_3 catalysts were prepared by the impregnation method according to the literature [29]. The precursors were obtained by the impregnation of aqueous solution of $RuCl_3$ into γ-Al_2O_3(2–4 mmϕ spheres). They were washed and dried, followed by reduction in N_2H_4 aqueous solution. Table 1 shows the characteristics of the catalysts (Ru-A, Ru-B) obtained by the above procedure. Before taking measurements of the CO PROX activity, further reduction of the Ru/Al_2O_3 in N_2 containing 9.5 vol.% H_2 flow was carried out for 2 h for the activation according to the literature [29].

Catalytic activity was measured in a fixed bed flow reactor made of a piece of stainless steel tubing (16.4 mm I.D.) under almost atmospheric pressure. At the center of the reactor, 8 ml (5.6 g) of each Ru/Al_2O_3 catalyst was placed. To measure the CO PROX activity, the temperature of the reactor was increased to the test temperature under an N_2 flow. The test gas, generated from standard gas by mass flow controllers, was fed at a flow rate of 1000 ml/min, corresponding to GHSV = 7500 h^{-1}. The GHSV value is shown in dry base. Water was added to the test gas by a pump through a vaporizer before the reactor. Reaction temperatures were measured by a thermocouple located along the centerline of the reactor. The maximum temperature of the catalyst layer, which was always at the top of the catalyst layer, is shown in the table and figures as the reaction temperature.

Table 1
Characteristics of Ru/Al_2O_3 samples

Notation	Ru loading (wt.%)	BET surface area (m^2/g-cat)	CO adsorption[a] (cm^2/g-cat)	Ratio of surface Ru(0)[b] (%)
Ru-A	1.01	174	1.35	7
Ru-B	0.93	175	1.07	1

[a]After reduction at 673 K.
[b]Without pre-treatment.

The gas compositions at the inlet and the outlet of the reactor at a stationary state were analyzed with a gas chromatograph equipped with TCD and FID. The results are shown in dry base. The detection limits of both CO and CH_4 were 0.5 ppm, while the detection limit of O_2 was 20 ppm. Concentrations below the detection limit are plotted as 0 ppm in the figures. The CO conversion was defined as (inlet CO−outlet CO)/(inlet CO). The selectivity was defined as {(inlet CO−outlet CO−outlet CH_4)/2}/(inlet O_2−outlet O_2).

The amount of CO adsorption on the catalyst was measured at 323 K by the pulse method. Before taking the measurement, the catalyst was reduced at a H_2 flow at 673 K for 45 min.

ESCA spectra were taken on the PHI 5700 ESCA system with the PC-ACCESS data analysis system (Physical Electronics Inc.). For the analysis of the catalysts after the tests, the samples were transferred from the reactor to the chamber under Ar atmosphere to avoid exposure to air. A catalyst sphere was set on a sample holder and it was introduced into the ultra high vacuum chamber. After the pressure in the chamber was lowered to below 10^{-6} Pa, the X-ray photoelectron spectroscopy was measured by using an Mg anode as the X-ray source. In the case of supported catalysts, electrons from the support can be used as an internal reference [31]. Therefore, the Al 2p line of 74.4 eV of the Al_2O_3 support was used as an internal reference for determination of the binding energies [32]. The peak separation of Ru 3d was carried out between 277.5 eV and 292.5 eV according to the previous report by Cattania et al. [33]. The binding energy of Ru $3d_{5/2}$ of Ru(0) was referred to be 280.2 eV [33], and the Ru in the oxidized state was separated into RuO_2, $RuO_2 \cdot xH_2O$ and $RuOx$. The binding energies of Ru $3d_{5/2}$ of RuO_2, $RuO_2 \cdot xH_2O$ and $RuOx$ were referred to be 280.7 eV [32], 281.4 eV [34] and 282.5 eV$\sim$ [32], respectively. The peaks of Ru $3d_{3/2}$ of Ru(0), RuO_2, $RuO_2 \cdot xH_2O$ and $RuOx$ were set according to the assumption that the ratio of the peak area of Ru $3d_{3/2}$ to Ru $3d_{5/2}$ was 2:3 and the binding energy of Ru $3d_{3/2}$ was shifted to 4.17 eV higher than that of Ru $3d_{5/2}$ [32]. $RuClx$ was not set in as the literature [33] because the Cl 2p peak was slight and it was difficult to assign trace $RuClx$ in the oxidized Ru. The binding energy of C 1s peak for adventitious hydrocarbon was set at between 284.6 eV and 285.0 eV [35, 36]. Moreover, C 1s peak for the carbon combined with oxygen was set at around 289 eV in some samples [32]. The ratio of Ru(0) to total Ru atoms on the surface of the catalyst was calculated as (peak area of Ru $3d_{5/2}$ of Ru(0))/(Ru $3d_{5/2}$ of Ru(0) + RuO_2 + $RuO_2 \cdot xH_2O$ + $RuOx$).

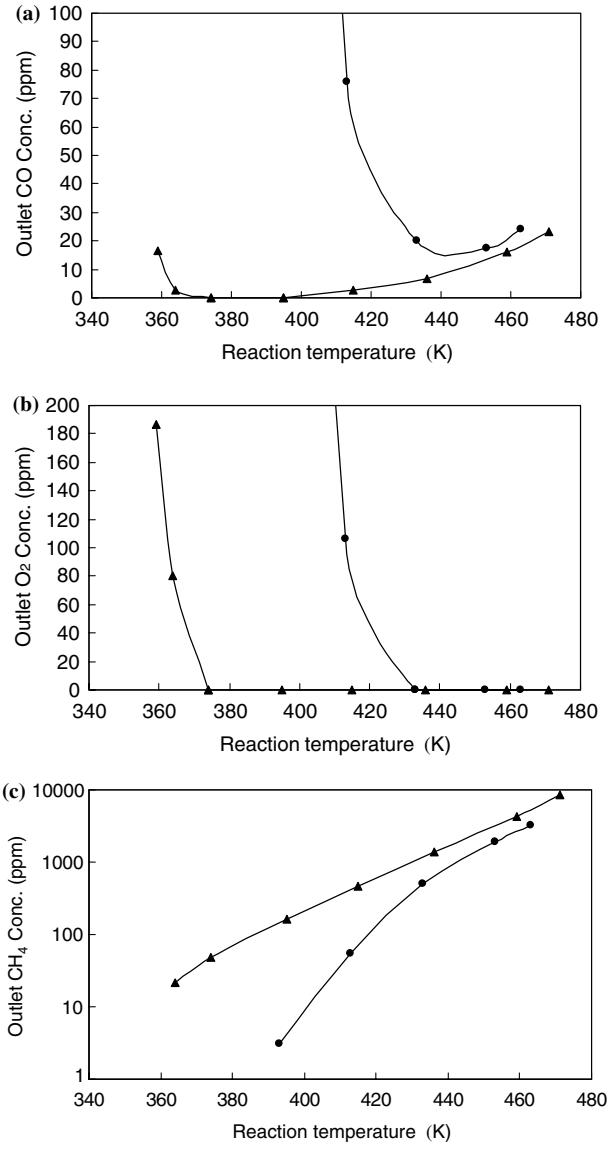

Figure 1. Comparison of the CO PROX activities of the non-activated catalyst and the activated catalyst at $[O_2]/[CO] = 1.5$; (a) Outlet CO concentration, (b) Outlet O_2 concentration, (c) Outlet CH_4 concentration. Reaction conditions: 0.5 vol.% CO, 20 vol.% CO_2, 0.75 vol.% O_2, 3 vol.% N_2, H_2 balance (dry base), 11 vol.% H_2O (wet base), GHSV = 7500 h^{-1} (dry base); (●) non-activated Ru-A, (▲) activated Ru-A.

3. Results

Figure 1 shows the temperature dependence of the CO PROX activity of the non-activated Ru catalyst and the activated Ru catalyst at $[O_2]/[CO] = 1.5$, where the Ru-A without any pre-treatment was used as the non-activated catalyst and the Ru-A, which was further reduced at 523 K in the H_2/N_2 gas as a pre-treatment, was used as the activated catalyst. As shown in figure 1(a), there was no temperature window where CO was reduced to below 10 ppm on the non-activated catalyst. In contrast, CO was removed to below 10 ppm

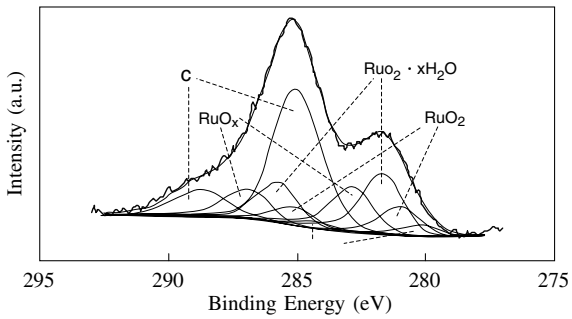

Figure 2. ESCA spectra for Ru 3d and C 1s of non-activated Ru-A catalysts.

between ca. 358 K and ca. 443 K on the activated catalyst. As for O_2 consumption, the outlet O_2 concentration for the non-activated catalyst decreased below the detection limit only at temperatures over 433 K. In contrast, the outlet O_2 concentration for the activated catalyst decreased below the detection limit at temperatures over 373 K, as shown in figure 1(b). It is known that methanation occurs as a side reaction in the CO preferential oxidation using a noble metal catalyst [7, 9]. At 373 K, CH_4 was not detected in the outlet of the non-activated catalyst, while 49 ppm CH_4 was detected in the outlet of the activated catalyst.The outlet CH_4 concentration of the activated catalyst was higher than that of the non-activated catalyst at all reaction temperatures, as shown in figure 1(c).

The change in oxidation state by this activation was analyzed using ESCA. As a non-activated catalyst, the Ru-A, which was once increased to 343 K in N_2 flow to replicate the warm-up period for the activity measurement, was analyzed. As an activated catalyst, the Ru-A, which was heated at 523 K for 2 h in the H_2/N_2 flow, was analyzed. Figures 2 and 3 show the ESCA spectra of the non-activated catalyst and the activated catalyst, respectively. The Ru on the activated catalyst has a more metallic character than that on the non-activated catalyst because the binding energy of Ru 3d of the activated catalyst was clearly shifted to a lower energy than that of the non-activated catalyst. In the case of the

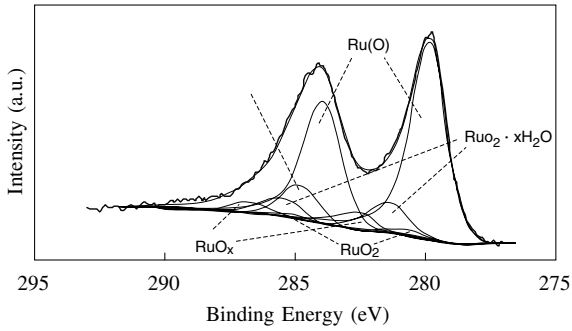

Figure 3. ESCA spectra for Ru 3d and C 1s of activated Ru-A catalysts.

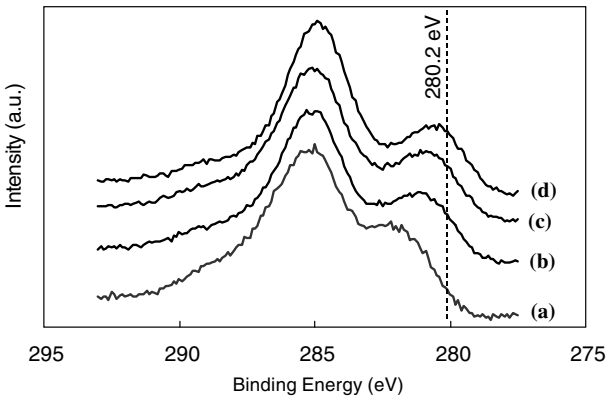

Figure 4. ESCA spectra for Ru 3d and C 1s of Ru-B catalysts; (a) Ru-B (without pretreatment), (b) Ru-B1, (c) Ru-B2, (d) Ru-B3.

activated Ru catalyst, the peak for Ru $3d_{5/2}$ of Ru(0) was set to be 279.9 eV for the peak separation. It is considered that the peak was shifted to the lower energy due to the effect of extra-atomic relaxation energy in the remarkable metallic circumstance [37]. The ratio of the surface Ru(0) of the activated catalyst was estimated to be 77%, while that of the non-activated catalyst was 8% by the peak separation.

The correlation between the CO PROX activity and the ratio of the surface Ru(0) of the catalyst was investigated. Before taking the measurements of the CO PROX activity, the Ru-B was heated in the H_2/N_2 flow at 323 K (Ru-B1), 343 K (Ru-B2) and 453 K (Ru-B3) for the pre-treatment. Figure 4 shows the ESCA spectra of these catalysts. The peak binding energy of Ru 3d was shifted to a lower energy as the pre-treatment temperature was increased. By the peak separations, the ratios of the surface Ru(0) were estimated to be 28% for the Ru-B1, 40% for the Ru-B2 and 53% for the Ru-B3, respectively. The CO PROX activities of these catalysts at $[O_2]/[CO] = 1.5$ are shown in tables 2, 3 and 4. As shown in table 2, the temperature window, where CO was reduced to below 10 ppm, was expanded to the lower temperature side as the surface Ru(0) ratio of the catalyst was increased. Moreover, both the minimum value of the outlet CO concentration and the temperature giving the minimum value lowered as the surface Ru(0) ratio of the catalyst was increased. As shown in table 3, as for O_2 consumption, the lower limit temperature at which O_2 was consumed below the detection limit was lowered as the surface Ru(0) ratio of the catalyst was increased. The outlet O_2 concentration below 423 K was higher in the order of Ru-B1 > Ru-B2 > Ru-B3. Regarding the methanation side reaction, the outlet CH_4 concentration was higher in the order of Ru-B3 > Ru-B2 > Ru-B1 at all temperatures, as shown in table 4. The selectivity for CO oxidation and the CO conversion of the catalysts at low temperatures are shown in table 5. Although the CO conversion decreased remarkably with decreasing the surface Ru(0) ratio at low temperatures, the selectivity hardly varied regardless of the change of the surface Ru(0) ratio.

In order to investigate the change of the activity and oxidation state of Ru under the CO PROX, the reaction

Table 2
Comparison of outlet CO concentrations on CO PROX at $[O_2]/[CO]=1.5$

Catalyst	Surface Ru(0) ratio (%)	Outlet CO concentration (ppm)					
		363 K	383 K	403 K	423 K	443 K	463 K
Ru-B1	28	3951	1880	364	13	9.5	19
Ru-B2	40	354	67	13	5.9	7.8	17
Ru-B3	53	49	5.9	3.6	4.2	8.2	19

Reaction conditions: 0.5 vol.% CO, 20 vol.% CO_2, 0.75 vol.% O_2, 3 vol.% N_2, H_2 balance (dry base), 11 vol.% H_2O (wet base), GHSV = 7500 h^{-1} (dry base).

Table 3
Comparison of outlet O_2 concentrations on CO PROX at $[O_2]/[CO]=1.5$

Catalyst	Surface Ru(0) ratio (%)	Outlet O_2 concentration (ppm)					
		363 K	383 K	403 K	423 K	443 K	463 K
Ru-B1	28	5945	2196	193	0	0	0
Ru-B2	40	810	177	0	0	0	0
Ru-B3	53	186	0	0	0	0	0

Reaction conditions: 0.5 vol.% CO, 20 vol.% CO_2, 0.75 vol.% O_2, 3 vol.% N_2, H_2 balance (dry base), 11 vol.% H_2O (wet base), GHSV = 7500 h^{-1} (dry base).

Table 4
Comparison of outlet CH_4 concentrations on CO PROX at $[O_2]/[CO]=1.5$

Catalyst	Surface Ru(0) ratio (%)	Outlet CH_4 concentration (ppm)					
		363 K	383 K	403 K	423 K	443 K	463 K
Ru-B1	28	0	0.6	41	718	2146	5577
Ru-B2	40	5	60	202	721	2182	5683
Ru-B3	53	35	144	387	941	2447	5791

Reaction conditions: 0.5 vol.% CO, 20 vol.% CO_2, 0.75 vol.% O_2, 3 vol.% N_2, H_2 balance (dry base), 11 vol.% H_2O (wet base), GHSV = 7500 h^{-1} (dry base).

Table 5
Comparison of selectivity and CO conversion

Catalyst	Surface Ru(0) ratio (%)	Selectivity[%](CO conversion [%])		
		363 K	383 K	403 K
Ru-B1	28	33.7 (21.0)	29.4 (62.4)	31.4 (92.7)
Ru-B2	40	34.7 (92.9)	33.3 (98.7)	31.9 (99.7)
Ru-B3	53	33.6 (99.0)	32.3 (99.9)	30.7 (99.9)

Reaction conditions: 0.5 vol.% CO, 20 vol.% CO_2, 0.75 vol.% O_2, 3 vol.% N_2, H_2 balance (dry base), 11 vol.% H_2O (wet base), GHSV = 7500 h^{-1} (dry base).

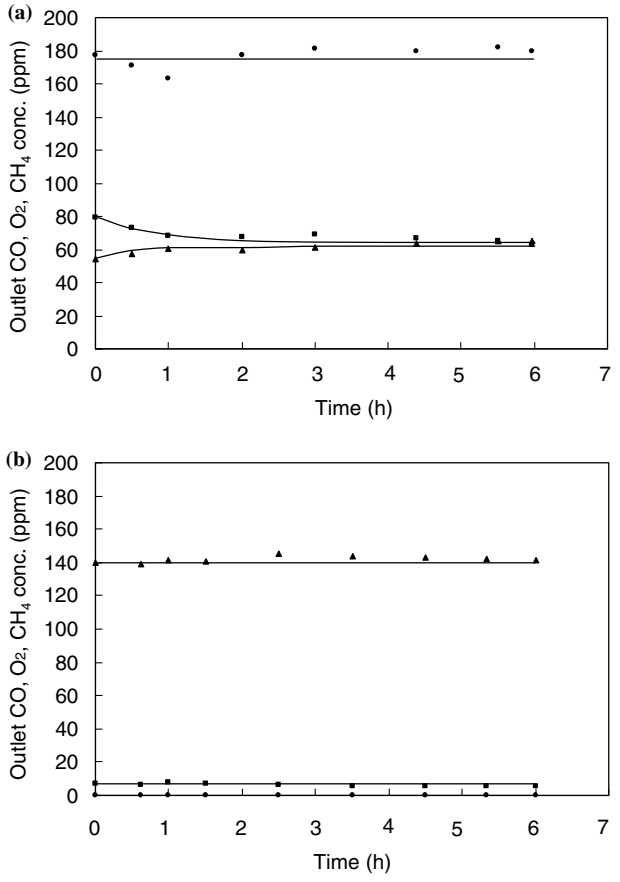

Figure 5. Stability of the CO PROX activities of Ru-B2 and Ru-B3 at $[O_2]/[CO] = 1.5$; (a) Ru-B2, (b) Ru-B3. Reaction conditions: 0.5 vol.% CO, 20 vol.% CO_2, 0.75 vol.% O_2, 3 vol.% N_2, H_2 balance (dry base), 11 vol.% H_2O (wet base), Temp. = 383 K, GHSV = 7500 h^{-1} (dry base); (■) Outlet CO concentration, (●) Outlet O_2 concentration, (▲) Outlet CH_4 concentration.

was carried out on the Ru-B2 and Ru-B3 at 383 K for 6 hours. Figure 5 shows the change of the activity. The outlet CO, O_2 and CH_4 concentrations of these catalysts were almost stable. Then the ESCA measurements were carried out for these catalysts after the CO PROX. By the peak separations, the ratios of the surface Ru(0) after the CO PROX were estimated to be 40% for the Ru-B2 and 54% for the Ru-B3, respectively. Thus, the ratios of the surface Ru(0) after the CO PROX were similar to those before the reaction at that temperature.

4. Discussion

As shown in figures 1(a), 2 and 3, on the activated Ru catalyst, in which 77% of surface Ru atoms were reduced to metal, CO was removed to below 10 ppm from the simulated reformed gas between ca. 358 and 443 K at $[O_2]/[CO] = 1.5$. Meanwhile, on the non-activated Ru catalyst, in which 8% of surface Ru atoms were reduced to metal, CO was not reduced to below 10 ppm at the low O_2/CO condition. Thus, the activated Ru catalyst that had a large population of Ru(0) on the surface showed high CO PROX activity. This result agrees with a previous report [38].

The temperature window, where CO was reduced to below 10 ppm, expanded to the lower temperature side with increasing the surface Ru(0) ratio of the Ru catalyst, as shown in table 2. Moreover, the lower limit temperature at which O_2 was consumed to below the detection limit lowered with increasing the surface Ru(0) ratio, as shown in table 3. The temperature corresponds to the lower limit temperature at which CO was reduced to ca. 10 ppm in the catalysts. This correspondence is also observed in the results shown in figures 1(a) and 1(b). Thus, complete O_2 consumption is considered to be required for the CO PROX removal below 10 ppm on the Ru catalyst at low temperatures. On the other hand, although the CO conversion increased with increasing the surface Ru(0) ratio at low temperatures, the selectivity for CO oxidation hardly varied with the change of the surface Ru(0) ratio, as shown in table 5. Therefore, it can be considered that the CO conversion of the Ru catalyst is dominated not by the selectivity but by the activity of CO oxidation by O_2 at low temperatures. Moreover, the activity of CO oxidation by O_2 at low temperatures improved with increasing the surface Ru(0) ratio of the catalyst. Consequently, it can be supposed that O_2 activation on Ru(0) is the key step for the CO PROX on the Ru catalyst at low temperatures.

There is concern that the oxidation state of surface Ru on the Ru/Al_2O_3 may change under the CO PROX conditions. However, it was confirmed that the oxidation state of the surface Ru were hardly changed under the CO PROX conditions at the low temperature, as mentioned above. There is also concern that the oxidation state of surface Ru on the Ru/Al_2O_3 may change under high vacuum pressure for ESCA measurement conditions. The ESCA measurements of the Ru-B and Ru-B2 were carried out after 6 hours and 72 hours from introduction into the vacuum system. Consequently, it was confirmed that the surface Ru was not further reduced under the high vacuum pressure. It can be supposed that the oxidation state of surface Ru on the Ru/Al_2O_3 measured by ESCA gives reliable information for characterizing the CO PROX catalyst.

As for the methanation side reaction, the outlet CH_4 concentrations increased with increasing the Ru(0) ratio on the catalyst surface at all temperatures, as shown in figures 1(c), 2, 3 and table 4. Considering the outlet CH_4 concentrations, it is clear that the most of the CO was removed by oxidation at low temperatures. However, there is a possibility that CO methanation assists the low outlet CO concentration of the activated Ru catalyst.

On the other hand, the support of the catalyst may influence the oxidation state of the Ru. Further investigations are required to clarify the influence.

5. Conclusion

The ratio of Ru(0) to total Ru on the surface of the Ru catalyst was increased by heating in a H_2/N_2 mixed gas after aqueous reduction. As the surface Ru(0) ratio of the CO PROX catalyst was increased, the temperature window, where CO was reduced to below 10 ppm, was expanded to the lower temperature side. The lower limit temperature at which O_2 was completely consumed corresponded to that at which CO was reduced to ca. 10 ppm on the catalyst. Although the CO conversion increased with increasing the surface Ru(0) ratio at low temperatures, the selectivity for CO oxidation hardly varied regardless of the surface Ru(0) ratio. It is supposed that the CO PROX activity of the Ru catalyst at low temperatures is dominated by O_2 activation on Ru(0) and the increase in the surface Ru(0) ratio by the H_2/N_2 reduction causes the high activity of the activated Ru catalyst.

References

[1] O. Okada, S. Takami, N. Iwasa, T. Ohhama and H. Yamamoto, Abstracts of 1992 Fuel Cell Seminar, Tucson, AZ, 29 Nov.–2 Dec. (1992) 473.
[2] M. Masuda, O. Okada, S. Takami, S. Nagase, N. Iwasa, T. Ohhama and H. Yamamoto, Abstracts of 1994 Fuel Cell Seminar, San Diego, CA, 28 Nov.–1 Dec. (1994) 380.
[3] O. Okada and K. Yokyama, Fuel Cells, 1 (2001) 72.
[4] S. Gottesfeld and J. Pafford, J. Electrochem. Soc. 135 (1988) 2651.
[5] L.A. Lemons, J. Power Sources 29 (1990) 251.
[6] H.-F. Oetjen, V.M. Schmidt, U. Stimming and F. Trila, J. Electrochem. Soc., 143 (1996) 3838.
[7] S. Kawatsu, S. Aoyama and M. Iwase, Abstracts of 1996 Fuel Cell Seminar, Orlando, FL, 17–20 Nov. (1996) 262.
[8] T.R. Ralph, G.A. Hards, J.E. Keating, S.A. Campbell, D.P. Wilkinson, M. Davis, J. St-Pierre and M.C. Johnson, J. Electrochem. Soc., 144 (1997) 3845.
[9] S. Kawatsu, J. Power Sources, 71 (1998) 150.
[10] H. Igarashi, H. Uchida, M. Suzuki, Y. Sasaki and M. Watanabe, Appl. Catal. A, 159 (1997) 159.
[11] Y. Gonjo, M. Sato and T. Sugimoto, Proceedings of the 2nd International Fuel Cell Conference, Kobe, Japan, 5–8 Feb. (1996) 359.
[12] C.D. Dudfield, R. Chen and P.L. Adcock, J. Power Sources 86 (2000) 214.
[13] C. Wunderlich and F. Reichenbach, Proceedings of the Fuel Cell Home, Lucerne, Switzerland, 2–6 July (2001) 133.
[14] S.H. Lee, J. Han and K.-Y. Lee, J. Power Sources 109 (2002) 394.
[15] M.A. Inbody, R.L. Borup and J.I. Tafoya, Abstracts of 2002 Fuel Cell Seminar, Palm Springs, CA, 18–21 Nov. (2002) 794.
[16] W. Yoon, C. Kim, M. Han, J. Park and J. Jeong, Abstracts of 2002 Fuel Cell Seminar, Palm Springs, CA, 18–21 Nov. (2002) 639.
[17] M. Watanabe, H. Uchida, H. Igarashi and M. Suzuki, Chem. Lett. (1995) 21.
[18] O. Korotkikh and R. Farrauto, Catal. Today 62 (2000) 249.
[19] H. Igarashi, H. Uchida and M. Watanabe, Chem. Lett. (2000) 1262.
[20] I.H. Son and A.M. Lane, Catal. Lett. 76 (2001) 151.
[21] H. Igarashi, H. Uchida and M. Watanabe, Stud. Surf. Sci. Catal. 132 (2001) 953.
[22] A. Manasilp and E. Gulari, Appl. Catal. B 37 (2002) 17.
[23] X. Liu, O. Korotkikh and R. Farrauto, Appl. Catal. A 226 (2002) 293.
[24] I.H. Son, M. Shamsuzzoha and A.M. Lane, J. Catal. 210 (2002) 460.
[25] S.H. Oh and R.M. Sinkevitch, J. Catal. 142 (1993) 254.
[26] N. Yamada, J. Koezuka, K. Takasu and M. Enami, Proceedings of the 4th FCDIC Fuel Cell Symposium, Tokyo, Japan, 15–16 May (1997) 129.
[27] C.D. Dudfield, P.L. Adcock and R. Chen, Abstracts of 1998 Fuel Cell Seminar, Palm Springs, CA, 16–19 Nov. (1998) 341.
[28] M. V. Twigg, *Catalyst Handbook, 2nd ed.*, (Wolfe Publishing Ltd., London, UK, 1989).
[29] M. Echigo and T. Tabata, Appl. Catal. A 251 (2003) 157.
[30] M. Echigo, N. Shinke, S. Takami and T. Tabata, J. Power Sources, 132 (2004) 29.
[31] A.M. Venezia, Catal. Today 77 (2003) 359.
[32] J.F. Moulder, W. F. Stickle, P. E. Sobol and K. D. Bomben, *Handbook of X-ray Photoelectron Spectroscopy*, Physical Electronics, Inc., Minnesota, (1992).
[33] M.G. Cattania, F. Parmigiani and V. Ragaini, Surf. Sci. 211 (1989) 1097.
[34] K.S. Kim and N. Winograd, J. Catal. 35 (1974) 66.
[35] S. Kohiki, J. Surf. Anal. 2 (1996) 187.
[36] S. Hashimoto, K. Hirokawa, Y. Fukuda, K. Suzuki, T. Suzuki, N. Usuki, N. Gennai, S. Yoshida, M. Koda, H. Sezaki, H. Horie, A. Tanaka and T. Ohtsubo, Surf. Interface Anal. 18 (1992) 799.
[37] S. Kohiki and S. Ikeda, Phys. Rev. B 34 (1986) 3786.
[38] S.F. Abdo, K.M. VandenBussche, D.R. Sioui, T. M. Mezza and S.R. Bare, Preprints of Papers. American Chemical Society. Fuel Chemistry Division 47 (2002) 549.